



21st IAEA Fusion Energy Conference  
Chengdu, China, 16 - 21 October, 2006

---

IAEA-CN-149/ EX/P4-27

## Quantitative Analysis of Plasma Particles in Materials Exposed to LHD Divertor Plasmas

M. Tokitani et al.

NIFS-847

Oct. 2006

## Quantitative analysis of plasma particles in materials exposed to LHD divertor plasmas

M. Tokitani 1), N. Yoshida 1), K. Tokunaga 1), T. Fujiwara 1), S. Masuzaki 2), N. Ashikawa 2), M. Shoji 2), T. Morisaki 2), M. Kobayashi 2), K. Nishimura 2), A. Sagara 2), N. Noda 2), H. Yamada 2), A. Komori 2), LHD experimental group 2), S. Nagata 3), B. Tsuchiya 3)

1) Research Institute for Applied Mechanics, Kyushu University, Kasuga, Fukuoka 816-8580, Japan

2) National Institute for Fusion Science, Oroshi, Toki, Gifu 509-5292, Japan

3) Institute for Materials Research, Tohoku University, Sendai, Miyagi 980-8577, Japan

e-mail contact of main author: tokitani@riam.kyushu-u.ac.jp

**Abstract.** Surface modification and hydrogen retention of a LHD divertor tile used for plasma experiments for 6 years were analyzed by using ion beam analytical techniques. Several clear divertor footprints were identified on the central area of the tile surface. This area is an so called erosion dominant area. While, on the both sides of the central area, surfaces were covered mainly with Fe and Ti, respectively. The amounts of hydrogen retention were strongly dependent on the chemical composition of the surface. In the Ti rich deposition layer appeared in the private side, very strong hydrogen trapping was detected. In contrast, Fe rich area in the opposite side, the retention was much lower than that of the normal carbon surfaces.

### 1. Introduction

The large helical device (LHD) is the largest heliotron type plasma machine equipped with superconducting helical magnetic coil systems. For heliotron-type configurations including LHD, plasma current is not necessary to form the magnetic configuration for plasma confinement. Therefore, they have an advantage of disruption-free steady state plasma operation. One of the features of the LHD magnetic configuration, which is called the helical divertor system, is the intrinsic divertor structure without additional divertor coils. The edge plasma characteristics of LHD are actively controlled by using stable helical divertor system [1]. This system has a large merit for erosion/deposition and hydrogen isotope retention study of the divertor materials in LHD [2].

The first wall and divertor plates of LHD are made of stainless steels (SUS316L) and isotropic graphite (IG-430U), respectively. IG-430U tiles were mechanically joined with bolts to the water cooled copper heat sinks [3]. In 1999, IG-430U divertor tiles were installed by replacing the initial stainless steel tiles and it was succeeded to reduce radiations from metallic impurities (Fe, Cr, and Ni) and increase the plasma stored energies [4]. However, graphite has disadvantages such as higher sputtering yield and higher retention of hydrogen isotopes than metals. Uncontrollable plasma density rise occurred long pulse discharges with cyclotron range of frequency (ICRF) heating in LHD due to hydrogen outgas locally induced by heating of the IG-430U divertor plate during a discharge [5]. Improved divertor module has been developed for efficient heat removal [6].

Therefore, quantitative data of retained plasma particles in the divertor plates is important for the steady state plasma operation as well as for tritium inventory in the future. Though the erosion and deposition of the divertor targets have been studied extensively in the LHD [2], quantitative analysis of plasma particles retained in the divertor materials has not been done

so far. In this paper, retained hydrogen atoms in a divertor tile used for the plasma experiments for 6 years was analyzed by using elastic recoil detection (ERD) analysis. Furthermore, the change of composite elements of the tile surface due to exposure of divertor plasmas was analyzed by using Rutherford backscattering spectrometry (RBS). The surface modifications of the tile surface were observed by scanning electron microscopy (SEM).

## 2. Experimental Procedures

### 2.1. Analyzed tile

For quantitative analysis of retained hydrogen atoms in the LHD divertor tile (IG-430U), one tile used for 6 years (49088 shot in total) near the inner port of the torus was selected for analysis. The pictures showing its feature and position in LHD are shown later in FIG. 2 together with other experimental data. In LHD, thermo couples were embedded in some divertor plates to monitor temperature [5]. The incident ion energy distribution at the divertor tile is shifted-Maxwellian (sheath-potential+ $T_i$ ). Main component of  $T_e$  and  $T_i$  at the tile were expected to be  $T_e \sim T_i = 10\text{-}20$  eV. Taking into account the sheath potential, the actual incidence energy of the plasma bombarding the tile is considered to be about 100-200 eV.

### 2.2. Ion beam analysis (ERD and RBS) and observation of the surface modification

Quantitative analyses of the retained hydrogen atoms in the tile were carried out by means of ERD. Furthermore, chemical composition at the surface was measured by RBS simultaneously. FIG. 1 illustrates simultaneous measurement technique of ERD and RBS. Depth profile of hydrogen atoms was measured successfully by using a helium ( $^4\text{He}^{2+}$ ) analyzing beam ERD technique with energy of 2.8 MeV. The incident angle of the beam was  $72^\circ$  to the normal of the specimen surface. The back scattered  $^4\text{He}$  atoms were detected with the RBS detector (solid state detector) placed at an angle of  $170^\circ$  to the incidence direction. The recoiled hydrogen atoms were detected by the ERD detector (solid state detector) at the angle of  $30^\circ$  to the analyzing beam direction. An Al film of  $12\ \mu\text{m}$  thick was placed in front of the ERD detector to absorb the He ions scattered from the specimen surface. Spot size of the analyzing beam was about 3.2 mm, so we could measure the line distribution of the retained hydrogen atoms with resolution of 3.2 mm. The analyzing direction is noted in FIG. 2.

Morphology and composition of the surface were analyzed with a SEM equipped with energy dispersive X-ray spectrometer (EDS).

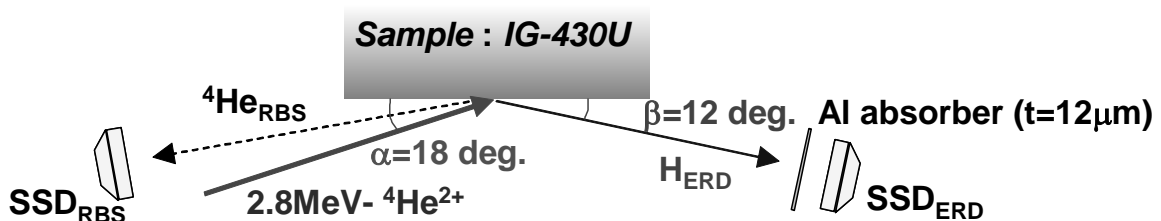


FIG. 1. Geometrical view of the simultaneous measurement technique of ERD and RBS.

### 3. Results and Discussion

#### 3.1. Chemical composition and surface modification on the IG-430U tile

Photographs in FIG. 2 show surface modification and position in LHD of the analyzed tile. Several clear divertor footprints were identified on the surface at the central area. They were caused by swinging the magnetic axis of the LHD plasma. FIG. 2 (i) shows the numerically calculated connection length profile of magnetic field line ( $L_c$ ) crossing the divertor plate for several magnetic axis positions ( $R_{ax}=3.5\sim 3.9$  m) [7]. These data indicate that the divertor strike points shift according with the change of the magnetic axis ( $R_{ax}$ ). Though operation at  $R_{ax}=3.75$ m is standard configuration, plasma experiments were often conducted at inward shifted configuration, for example at  $R_{ax}=3.6$  m, because the plasma performance at  $R_{ax}=3.6$  m was better than that at  $R_{ax}=3.75$  m [8]. Therefore, total influx of hydrogen on the right-hand side area (private side) is lower than that of the left-hand side area. For convenience these sides are denoted inner side and outer side, respectively, in this paper.

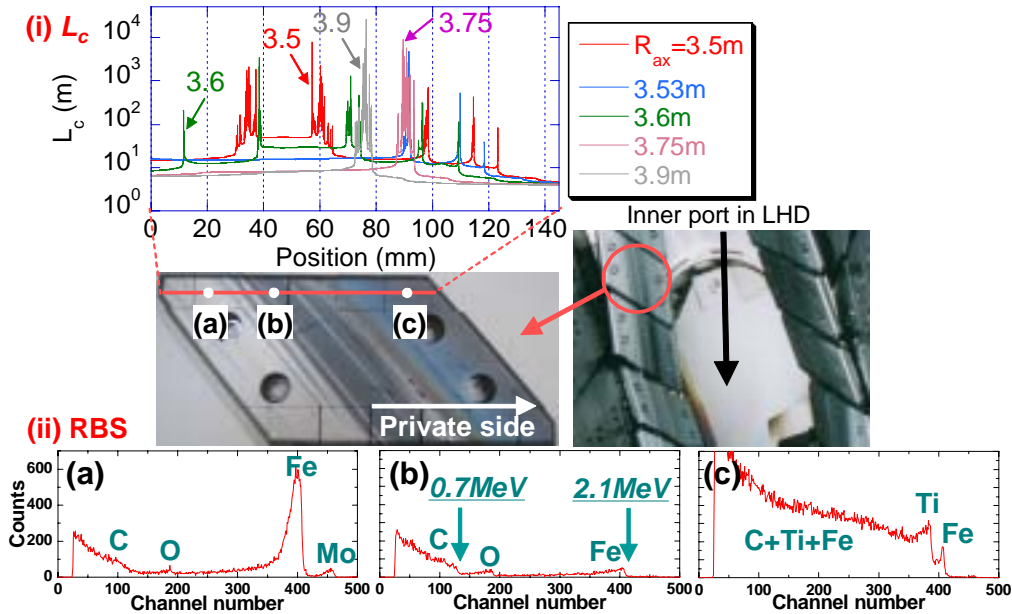


FIG. 2. (i) Connection lengths of magnetic field lines ( $L_c$ ) for the case of the several magnetic axis ( $R_{ax}=3.5\sim 3.9$  m). The peak of  $L_c$  corresponds to the divertor strike points. (ii) Chemical composition of deposits by RBS, channel number corresponds to the energy of the back scattered  $^4\text{He}$  beam.

The central area of the divertor, where many footprints exist, is still keeping graphite color (black), but the inner side (private side) has changed to brown or blue and the outer side is glossy metallic color. These results indicate that the central area is erosion dominant while the areas on both sides are deposition dominant. Data of RBS corresponding to the positions of (a), (b) and (c) in the photograph are illustrated in FIG. 2 (ii). The channel number in the figure corresponds to the energy of the back scattered  $^4\text{He}$  atoms. For example, channel number 410 corresponds to 2.1 MeV as noted in (b). As shown by the RBS data, chemical composition at the surface is very position dependent. Namely, outer side (point (a)) was mainly covered by deposited Fe layer. The width of the Fe peak indicates that the thickness of

the Fe layer is about 16 nm. It seems that the Fe impurities came from the first wall during glow discharge cleaning (GDC) [9]. Fe atoms also deposit on the central area surface, point (b), but it is very thin. In contrast, not only Fe but also large amount Ti are deposited in the right-hand side area, point (c). High counts between 100 and 350 channel indicates that a mixed materials composed of C, Ti, Fe and O of about a few hundred nm thick is formed on the inner side surface. This layer is a kind of co-deposition layers which have been observed in many fusion experimental devices [10-13]. In LHD, Ti gettering is often used to reduce oxygen impurities in the vacuum vessel [4]. It is likely that Ti getting rids of sputtering erosion remained on the surface. EDS analysis indicated that substantial amounts of O and C were also deposited together with Ti and Fe.

Surface morphology of the tile observed by SEM is shown in FIG. 3. Surface at the outer side, (a), looks relatively smooth. This fact indicates that strong sputtering erosion has not occurred at this area. The porous surface at the central area, (b) indicates strong sputtering erosion. The surface of the inner side are covered by deposits with small hills of about 1-2  $\mu\text{m}$  in size. In this area, it is consider that not only the deposition but also the erosion is simultaneously occurred, and due to these repetitions this type structure was finally formed. This is a kind of co-deposition layer. As mentioned above, the RBS data of FIG. 2 (ii) indicate that mixed material composed of C, Ti, Fe and O of about a few hundred nm thick is formed on the surface of the (c).

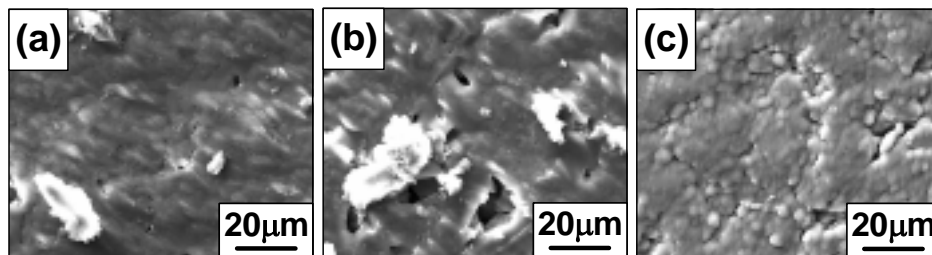


FIG. 3. SEM micrograph of IG-430U. Position (a), (b) and (c) correspond to those of FIG. 2

### 3.2. Retention of hydrogen

ERD analyses were performed along the line crossing the footprints as drawn in the photograph of FIG. 2. Estimated areal density of hydrogen is plotted in FIG.4 against position. Retention of hydrogen is lowest ( $\sim 1 \times 10^{21} \text{ H/m}^2$ ) at the outer side, where Fe deposits covered the surface. In the central area, erosion dominant area, retained hydrogen is about  $3 \times 10^{21} \text{ H/m}^2$ . On the other hand, in the inner side (private side), which was covered by a thick co-deposition of Ti, Fe, C and O, hydrogen retention is highest ( $\sim 5 \times 10^{21} \text{ H/m}^2$ ). Depth profiles of the retained hydrogen atoms at the points (a), (b) and (c) denoted in FIG. 4 are plotted in FIG. 5. In all cases, concentration of hydrogen is decreased with decreasing depth up to the depth of less than 100 nm. It is expected that retained hydrogen just beneath the

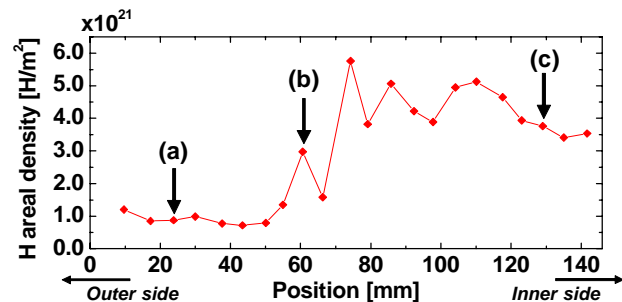


FIG. 4. Areal density of retained hydrogen atoms in IG-430U. The position of (a), (b) and (c) corresponds to those of FIG. 2.

tile surface (0-100 nm) was easily released due to the local temperature rise of sub-surface region. In cases of (b) and (c), concentrations of the hydrogen (H/C) reach  $\sim 0.3$  at the depth of 100-200 nm. This value is very close to the saturation level of hydrogen retention in graphite. Particularly in (c), large amount of hydrogen retained even in the deep area far beyond 500 nm. While, peak value of H/C for (a) is about  $\sim 0.15$ . It is likely that the deposition of Fe reduces the retention of hydrogen.

Judging from the connection length profile of the magnetic field lines (see FIG. 2 -(i)), and some probe measurements [1], influx of hydrogen on the inner side area is lower than that of the outer side. Nevertheless retained hydrogen is 4-5 times higher in the inner side. This fact implies that the retention of hydrogen does not simply depend on its influx, but change of surface properties due to impurity deposition is important factor determining hydrogen retention.

In the outer side, we can expect that Fe deposits prevent the retention of hydrogen. Injected hydrogen stop in the Fe deposits (thickness of 16 nm), because the projected range of 200 eV- $H^+$  in Fe is only about 4 nm. Furthermore, hydrogen injected in the Fe deposits will be released easily from the surface, because the trapping of hydrogen in Fe is weak [14], and thus the amount of hydrogen diffusing into the graphite tile decrease. On the other hand, one of possible explanations for the highest hydrogen retention in the inner side is following. It is likely that deposited Ti acts as very strong trapping site for hydrogen, because it forms very stable hydride. Large amount of hydrogen are trapped in the thick deposits by binding with Ti and C. Another possible explanation is that hydrogen atoms were trapped by between the interstitial positions of the complicated structure which was called co-deposition layer as shown in FIG. 3 (c). The shape of the ERD spectrum of (c) is intrinsically different from (a) and (b). In cases of (a) and (b), clear peak tops of hydrogen concentration are observed at the depth of 100-200 nm and then, these are quickly decreased with increasing depth from the surface. But, in the case of (c), the clear peak top has not been confirmed, and higher hydrogen concentration than (a) and (b) is kept beyond 500 nm from the surface. This result indicates that injected hydrogen atoms were diffused far deeper than the project range of the 200 eV- $H^+$  ( $\sim 4$  nm), through the co-deposition layer and finally, they were trapped as uniformly along the depth direction by the interstitial position of the thick co-deposits. Namely, as long as carbon co-deposition layer continues being formed, the retention capability of hydrogen isotopes of tile surface is not saturated. In Tore Supra, which uses carbon fiber composites (CFCs) for in-vessel components, very high hydrogen retention (D/C $\sim 0.4$ ) by the carbon co-depositions has been reported [15].

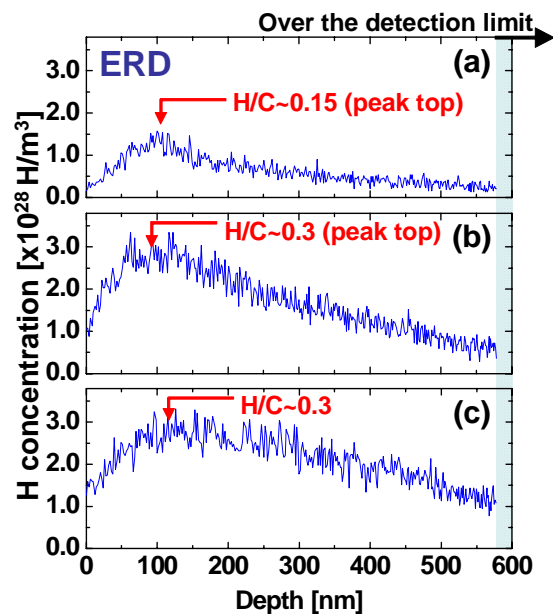


FIG. 5. Depth profile of the retained hydrogen atoms in IG-430U, each figure correspond to those of FIG. 4.

Present results indicate that physical and chemical properties of the plasma facing surface change from place to place depending on its position due to the complicated geometrical structure of the torus, use of different materials for each plasma facing component and a variety of discharge conditions including glow discharge cleaning and Ti gettering. Detailed information about the surface properties at the various places is necessary for the precise control of global particle balance as well as for the estimation of hydrogen inventory.

#### 4. Summary

To investigate the retention properties of plasma particles in LHD divertor tiles, hydrogen atoms retained in a divertor tile were analyzed by using ERD, and also the change of chemical properties and surface morphologies on the tile surface due to exposure of divertor plasmas were analyzed by using RBS and SEM, respectively.

From the experimental results, the amounts of hydrogen retentions were strongly dependent on the physical and chemical properties of the divertor surfaces. Especially, the inner side (c) in FIG. 2, very high amount of hydrogen retention was observed ( $\sim 5 \times 10^{21}$  H/m<sup>2</sup>). Depth profile of the hydrogen at (c) has been keeping constantly with the amount of  $2 \sim 3 \times 10^{28}$  H/m<sup>3</sup> even in the deep area far beyond 500 nm. Concentration of the hydrogen (H/C) at the depth of 100-200 nm has reached near the saturation level (H/C $\sim$ 0.3) of the carbon materials. One of the possible reasons of the highest hydrogen retention as compared with the (a) and (b) in FIG. 2 is that deposited Ti may act as very strong trapping site for hydrogen, because it forms very stable hydride. Another possible reason is that hydrogen atoms were trapped by between the interstitial positions of co-deposition layer. In contrast, the outer side (a), Fe rich layer can decrease the amount of the hydrogen retention than that of the normal carbon surfaces. It is considered that hydrogen injected in the Fe deposits will release easily from the surface, because the trapping of hydrogen isotope in Fe is weak [14]. In the central area (b), erosion dominant area, retained hydrogen is about  $3 \times 10^{21}$  H/m<sup>2</sup>. Concentration of the hydrogen (H/C) at the depth of 100-200 nm has reached  $\sim$ 0.3 as well as the inner side (c).

Considering the problem of a tritium inventory in the future, we should pay special precaution to the surface conditioning of the carbon divertor tile as well as the first wall. Therefore, presents data will be useful not only for evaluation of the divertor materials but also for proposal of the more effective wall conditioning method in LHD divertor tiles including hydrogen isotope removal.

#### Acknowledgements

This work was performed with the support and under the auspices of the NIFS Collaborative Research Program (Research code: NIFS04KLPP003) and under the inter-university cooperative research program of the Institute for Materials Research, Tohoku University. This research was partly supported by the Japan Society for the Promotion of Science and Grant-in-Aid of Scientific Research from Japan Ministry of Education, Culture, Sports, Science and Technology (JSPS Fellow-ship No.17-6042).

## References

- [1] S. Masuzaki et al., Nucl. Fusion 42 (2002) 750-758
- [2] A. Sagara et al., J. Nucl. Mater. 313-316 (2003) 1-10
- [3] N. Noda et al., Nucl. Fusion 41 (2001) 779
- [4] K. Nishimura et al., J. Nucl. Mater. 337-339 (2005) 431-435
- [5] M. Shoji et al., J. Nucl. Mater. 337-339 (2005) 186-190
- [6] Y. Kubota et al., Fusion Eng. Des. 75-79 (2005) 297-301
- [7] T. Morisaki et al., Contrib. Plasma. Phys. 40 (2000) 3-4, 266-270
- [8] O. Motojima et al., Nucl. Fusion 42 (2003) 1674-1683
- [9] M. Tokitani et al., Nucl. Fusion 45 (2005) 1544-1549
- [10] N. Bekris et al., J. Nucl. Mater. 313-316 (2003) 501-506
- [11] C. Brosset et al., J. Nucl. Mater. 337-339 (2005) 664-668
- [12] K. Masaki et al., J. Nucl. Mater. 337-339 (2005) 553-559
- [13] T. Hayashi et al., J. Nucl. Mater. 349 (2006) 6-16
- [14] M. Miyamoto et al., J. Nucl. Mater. 313-316 (2003) 82-86
- [15] J. Jacquinet et al., Nucl. Fusion 43 (2003) 1583-1599